ADVANCED THERAPEUTICS
www.advtherap.com

# Impact of Crystalline and Amorphous Matrices on Successful Spray Drying of siRNA Polyplexes for Inhalation of Nano-in-Microparticles

*Tobias W. M. Keil, Christoph Zimmermann, Domizia Baldassi, Friederike Adams, Wolfgang Friess, Aditi Mehta, and Olivia M. Merkel**

**To develop stable and inhalable dry powder formulations with long shelf life, polyplexes consisting of siRNA and a polyethylenimine (PEI)-based block copolymer in presence of mannitol or trehalose are spray dried. The effect of inlet (T-In) and outlet (T-Out) temperature on the recovery of siRNA and adsorption effects within the tubing material are investigated. Choosing a low abrasion silicon tubing prevented siRNA loss due to adsorption. Mannitol and trehalose formulations preserved siRNA integrity regardless of excipient concentration and temperature at T-Out below the siRNA melting temperature. Trehalose formulations allowed full siRNA recovery whereas mannitol formulations resulted in spray drying induced losses of ≈20% siRNA and of 50–60% polymer. Mannitol formulations showed optimal aerodynamic characteristics as confirmed by next generation impaction analysis based upon siRNA content. All spray dried formulations resulted in green fluorescent protein (GFP) silencing comparable or better than freshly prepared polyplexes. To test if the observed results could be transferred, formulations of siRNA and transferrin-PEI conjugates are spray dried, characterized, and used to transfect primary human T cells ex vivo. Results confirmed successful silencing of the transcription factor GATA3 in primary $CD4^+$ T cells with spray dried formulations as a potential treatment for severe asthma.**

## 1. Introduction

Local drug delivery to their site of action generally allows to reduce doses and side effects. For lung diseases such as Coronavirus Disease 2019 (COVID-19), COPD or asthma, pulmonary delivery is therefore favored.[1] With a relatively low enzyme activity and a slow surface clearance in the lung,[2] enzymatically prone substances specifically benefit from this administration route. In addition, dry powder inhalers enable the delivery of drugs with a long shelf life and also provide an easy to use tool for patients along with high compliance.[3] Despite several available treatments for lung diseases, RNA therapeutics have revolutionized how we treat previously uncontrollable diseases such as COVID-19 and hold promise for a variety of other diseases, such as severe, uncontrolled asthma.[4] Small interfering RNA (siRNA) can silence the translation of messenger RNA into disease causing proteins and can thus ameliorate symptoms or even interfere with viral infection.[5] However, siRNA therapeutics face several challenges associated with the delivery into cells and their enzymatic stability. To address these issues, nanoparticles are preferred for protecting and encapsulating siRNA. Numerous vehicles are reported in the literature to achieve uptake and transfection of cells with siRNA.[6] However, the only clinically approved siRNA drugs target the liver,[7] and inhalation delivery despite its many advantages has not yet reached clinical phase III.

Cationic polymers are one class of nucleic acid nanocarriers amongst which polyethylenimine (PEI) is the most studied example. However, the use of PEI is limited due to its cytotoxicity profile. To overcome toxic characteristics of PEI, our group has developed copolymers of PEI with better safety profiles. These copolymers combine nucleic acid condensation and protection efficiency of PEI with the advantage of amphiphilic materials for endosomal escape and the steric shielding effects of polycaprolactone (PCL) and polyethyleneglycol (PEG), respectively. It was shown that copolymers of (mPEG-b-PCL)-g-PEI (PPP) form so called polyplexes with nucleic acids in the nanoscale by electrostatic interaction and successfully transfect cells in vitro and in

Dr. T. W. M. Keil, C. Zimmermann, D. Baldassi, F. Adams, Prof. W. Friess, Dr. A. Mehta, Prof. O. M. Merkel
Department of Pharmacy, Pharmaceutical Technology and Biopharmacy
Ludwig-Maximilians Universität München
Munich 81377, Germany
E-mail: olivia.merkel@lmu.de
Dr. A. Mehta, Prof. O. M. Merkel
Comprehensive Pneumology Center Munich (CPC-M)
Ludwig-Maximilians Universität München
Munich 81377, Germany
Dr. A. Mehta, Prof. O. M. Merkel
German Center of Lung Research (Deutsches Zentrum für Lungenforschung, DZL)
Ludwig-Maximilians Universität München
Munich 81377, Germany

The ORCID identification number(s) for the author(s) of this article can be found under https://doi.org/10.1002/adtp.202100073



**DOI: 10.1002/adtp.202100073**

vivo.[8] In order to deliver these nanoparticles to the lung, incorporation into microparticles with aerodynamic diameters between 1 and 5 µm is required. The matrices of these microparticles need to consist of excipients which readily dissolve upon impact on lung lining fluid to release their nano-sized cargo.[9] The use of water soluble substances is hence required.

A technique to produce such nano-in-microparticles (NIM) is spray drying. It is a widely applied method in food, cosmetic, chemical and pharmaceutical industry and allows gentle drying of small droplets.[10] In addition, it is much faster and less time and energy consuming than spray freeze drying which is also used for the production of potential inhalable dry powder formulations of siRNA therapeutics.[11] However, spray drying applies heat to samples and might degrade or inactivate siRNA and/or its nanocarriers.[9] Also, pumping is a necessary step to process and ultimately spray samples. Here, adsorption based upon hydrophobic interactions between polyplexes and tubing surface could harm the formulation as was shown for DNA and a hydrophobized silica surface.[12] Furthermore, it is known that drying of biopharmaceuticals in combination with different excipients leads to amorphous or crystalline microparticles structures, depending on the nature of the excipient. This has tremendous effects on the stability and activity of the drug itself.[13] We hypothesized, that similar processes can also affect polyplexes and their composition.

Therefore, the aim of this study was to evaluate the highest possible inlet temperature to dry siRNA-PPP polyplexes in respect to quantity and integrity of the recovered nanoparticles. Importantly, quantification of siRNA upon polyplex redispersion after spray drying presents a novelty in the current literature. So far, this aspect has been disregarded in the siRNA formulation field, and we were the first to describe quantification of DNA upon polyplex redispersion of dry powders and transferred this knowledge within the work described here to siRNA polyplexes.[9] Additionally, we investigated absorption effects of standard silicon tubings in comparison to low abrasive silicon tubings, namely Pumpsil. Furthermore, we observed the effects of two different excipients, mannitol and trehalose, which are known to crystallize or form an amorphous state during spray drying, respectively. We investigated their effect at two different concentrations, i.e., 5 and 10% w/v feed solution, at the two highest possible temperatures where no negative impact on siRNA quantity and integrity was detected. All prepared formulations were characterized regarding their nanoparticle size and content, microparticle size (geometric and aerodynamic), residual moisture and crystallinity. Also, this study presents, for the first time, the determination of aerodynamic characteristics based on drug content as demanded by pharmacopoeias[14] and not via surrogate parameters as described by various other groups.[11,15]

Ultimately, freshly prepared and spray dried formulations were tested in vitro in an eGFP expressing cell line to confirm siRNA bioactivity after spray drying via eGFP silencing. To test if the observed results could be transferred to other siRNA polyplexes, formulations of siRNA against the pro-inflammatory Th2 transcription factor GATA3 and transferrin-PEI conjugates, a delivery system previously described by us,[16] were spray dried, characterized and assessed in a pharmacologically more relevant *ex vivo* model of GATA3 silencing in primary $CD4^+$ T cells.

## 2. Experimental Section

### 2.1. Materials

Double stranded siRNA targeting green fluorescent protein (DsiRNA EGFP 1) (siGFP) and scrambled non-specific control (siNC) were purchased from IDT (Integrated DNA Technologies, Inc., Leuven, Belgium). Branched polyethylenimine (PEI) (10 kDa) was obtained from Sigma Aldrich and 5 kDa PEI (Lupasol G100) was obtained from BASF (Ludwigshafen, Germany). Methoxy polyethylene glycol (mPEG-OH, 2000 g $mol^{-1}$) was acquired from TCI Germany. $\epsilon$-Caprolactone and $Sn(Oct)_2$ were purchased from Sigma-Aldrich and were freshly distilled ($\epsilon$-Caprolactone: distilled over $CaH_2$, $Sn(Oct)_2$: Kugelrohr distillation) prior to use. Heparin from porcine intestinal mucosa (H3393, >180 units $mg^{-1}$, grade I-A), 2,4,6-trinitrobenzesulfonic acid (TNBS) (P2297), TRIS EDTA Buffer Solution 1× (TE-buffer) (93283), TRIS EDTA Buffer Solution 100× for NGI analysis (T9285), tris borate EDTA buffer (TBE-buffer) (T 3913), RPMI-1640 Medium (R8758), fetal bovine serum (FBS) (F9665), Penicillin-Streptomycin (P/S) (P4333), G 418 disulfate salt solution (G8168), Dulbecco's Phosphate Buffered Saline (PBS) (D8537) and D-Mannitol, and human holo-transferrin (616397) were purchased from Merck KGaA (Darmstadt, Germany). D(+)-Trehalose dihydrate (28719.290) was acquired from VWR International GmbH (Darmstadt, Germany). Black and white 96 well plates (10307451), GeneRuler Ultra Low Range DNA Ladder (10400280), SYBR Safe DNA-Gel staining and polyacrylamide gels (Novex TBE Gels, 4–20%, EC62252BOX), and *N*-succinimidyl 3-(2-pyridyldithio) propionate (SPDP, 21857) were bought from Fisher Scientific (Schwerte, Germany). SYBR Gold dye was obtained from Life Technologies (Carlsbad, CA, USA). Pumpsil tubings were received as a kind gift from Watson-Marlow GmbH (Rommerskirchen, Germany) and had an inner diameter and a thickness of 1.6 mm.

### 2.2. Polymer Synthesis

Polymer synthesis was performed as described before.[16,17] In brief, mPEG-PCL-OH was synthesized via ring-opening polymerization of $\epsilon$-Caprolactone using $Sn(Oct)_2$ as catalyst and mPEG-OH as macroinitiator. For this ring-opening polymerization, 500 mg of mPEG-OH (2000 g $mol^{-1}$, 0.25 mmol, 1.0 eq.) were weighted into a heat-dried screw cap vial in a glovebox. Subsequently, 295 mg $\epsilon$-caprolactone (2.58 mmol, 10 eq., targeted polymer: mPEG(2000 g $mol^{-1}$)-PCL(1000 g $mol^{-1}$)) and 101 mg $Sn(Oct)_2$ (0.25 mmol, 1.0 eq.) were added, the vial was sealed and transferred to a heating block equipped with a magnetic stirrer preheated to 135 °C. The polymerization was conducted for 24 h at this temperature and was stopped by removal of the vial from the heating block, subsequent exposure to air, and dissolving of the very viscous oil in 2 mL of deuterated chloroform. An aliquot was taken from the reaction mixture to measure the conversion via $^1$H-NMR spectroscopy. After verification of full conversion (see Figure S1, Supporting Information), mPEG-b-PCL-OH was precipitated twice from cold diethyl ether, isolated via centrifugation and dried overnight in a vacuum oven at 65 °C. Successful synthesis, molar mass, and polydispersity of the copolymer were determined by GPC analysis (Figure S2,

Supporting Information) and $^1$H-NMR spectroscopy (Figure S3, Supporting Information). The molecular weights of the mPEG and PCl blocks were calculated by setting the number of protons of the mPEG methoxy group to 3. For the targeted polymer composition mPEG(2000 g mol$^{-1}$)-PCL(1000 g mol$^{-1}$), an accurate molar mass of mPEG(2100 g mol$^{-1}$)-PCL(1050 g mol$^{-1}$) was calculated. mPEG-PCl-acrylate was synthesized according to literature[18] using toluene instead of benzene. NMR spectra were recorded on a 300 MHz Varian Mercury Nuclear Magnetic Resonance (NMR) Spectrometer. Chemical shifts are given in ppm relative to the residual proton signal of deuterated chloroform. GPC chromatography was performed using a PL-50 SEC system with an RI-detector and two Agilent PL Gel 5 µm Mixed C (300 × 7.5 mm) columns. THF stabilized with 250 ppm BHT was used as the eluent at 35 °C with a flow rate of 1.0 mL min$^{-1}$. Polystyrene standards were used for column calibration.

The triblock copolymer polyethylenimine-*graft*-(polycaprolactone-*block*-methoxy-polyethylene glycol) (mPEG-b-PCL)-g-PEI) (PPP) was synthesized by coupling mPEG(2100 g mol$^{-1}$)-PCL(1050 g mol$^{-1}$) (6 eq.) to branched 10 kDa PEI (1 eq.) using a synthesis procedure from literature.[18] Using $^1$H-NMR spectroscopy, a grafting density of 4.9 was calculated (PEG = 40 mol%, PCL = 20 mol%, PEI = 40 mol%) with help of the ratio of the polymer signals of PEI, PEG, PCL and the methoxy-PEG groups resulting in the following polymer: (mPEG(2100 g mol$^{-1}$)-b-PCL(1050 g mol$^{-1}$))$_{4.9}$-g-PEI(10 000 g mol$^{-1}$) (Figure S4, Supporting Information). The transferrin conjugate (Tf-PEI) was obtained by coupling 5 kDa PEI with an excess of SPDP and mixing with activated SPDP-coupled transferrin as described before.[16] Characterization was performed by $^1$HNMR and UV spectroscopy as described before.[8b]

### 2.3. Polyplex Preparation

Stock solutions of siRNA and polymer were prepared at a concentration of 100 × 10$^{-6}$ M and 1 mg mL$^{-1}$, respectively. Polyplexes were prepared with a total amount of 30 µg of siRNA. Therefore, the amount of PEI ($m_{PEI}$) in µg was calculated as follows:

$$m_{PEI} = \left(\frac{m_{siRNA}}{M_{siRNA}}\right) \cdot 43.1\text{g mol}^{-1} \cdot \text{N/P} \quad (1)$$

whereas 43.1 g mol$^{-1}$ is the molecular weight of the so-called "protonable unit" (–CH$_2$–CH$_2$–NH–) of PEI, and N/P is the ratio of protonable amines (from PEI) per phosphates in the backbone of the RNA in the formulation. To calculate the masses required for each PEI derivative (i.e., PPP or Tf-PEI), the mass obtained for PEI was divided by the PEI weight content in the overall polymer.

The calculated amount of polymer was diluted up to 250 µL in a specified solvent (highly purified water (HPW), trehalose or mannitol, 5 or 10%), and 250 µL of the same solvent containing 30 µg siRNA were added. To allow polyplex formation, the mixture was incubated for 10 min. Then, 4500 µL of the same specified solvent was added and the polyplex suspension was incubated for another 10 min.

### 2.4. Adsorption to Tubing Material

In order to test whether adsorption of polyplexes to tubing material takes place during pumping, different tubing materials were washed prior to experiments with pre-heated HPW and allowed to dry. After insertion into the Masterflex L/S (7520-47, Cole-Parmer GmbH, Wertheim, Germany), equipped with the Easy-Load II head module (77201-60), a pump rate of 1.2 mL min$^{-1}$ was set. Polyplexes were prepared in HPW and pumped through the tubing and collected in a 5 mL tube for further analysis. This procedure was carried out in triplicates.

### 2.5. Spray Drying

For microparticle preparation a B-290 (Büchi Labortechnik, Essen, Germany) was used. As Pumpsil tubings did not fit into the Büchi pre-installed pump, the Masterflex L/S (see Section 2.4) was used with a pump rate of 1.2 mL min$^{-1}$. Nitrogen was used as atomizing gas, whereas drying gas was air. In order to avoid dust and other airborne particles, both nitrogen and air supply were filtered through a 0.22 µm pore. To ensure sufficient heating of the air supply and to avoid overheating of the Büchi vacuum pump, pressurized air was used. The aspirator was set to 70%, and vacuum was set to −42 mbar by adjusting the level of pressurized air. The airflow was set to 40 mm corresponding to 473 NL h$^{-1}$. For particle collection, a high efficiency cyclone was attached. Polyplexes were prepared in 5% or 10% w/v trehalose or mannitol. All formulations were prepared the same day to avoid inter-day differences related to ambient temperature and humidity, for example. For analysis, three batches were produced on three different days. In the case of different inlet-temperatures (T-In), the measured outlet-temperatures (T-Out) were indicated next to T-In for a better understanding of the process. During the spray drying process, minor changes of T-Out were observed. Hence, T-Out was reported as mean with a deviation of ± 1.5 °C.

### 2.6. Z-Average and PDI Measurements

To compare the effects of pumping and spray drying on polyplex content, 70 µL of freshly prepared polyplex suspension was compared to polyplexes after further processing. For pump adsorption experiments, 70 µL were taken after pumping. For redispersability of spray dried formulations, ≈3.5 mg and 7.0 mg for 5% and 10% matrix formulations, respectively, were dissolved in 70 µL HPW. All samples were analyzed in disposable cuvettes (Brand GmbH, Wertheim, Germany) and analyzed with the Zetasizer Nano ZS (Malvern Instruments Inc., Malvern, UK). Therefore, the refractive index of water, mannitol or trehalose at 25 °C for the indicated concentrations were set in the software, and detection was performed with the backscatter angle of 173°. For each experiment, measurements were taken in triplicates with 15 runs each and averaged afterwards.

### 2.7. Static Light Scattering

A few µg of spray dried powder was suspended in about 2 mL of diethyl ether. About 30 min prior to measurements

the HORIBA LA-950 (Retsch Technology GmbH, Haan, Germany) was switched on for equilibration. The cuvette was filled with diethyl ether, inserted into the device, and acquisition and blank measurements were recorded. The sample suspension was mixed thoroughly by pipetting up and down, and small amounts were added into the cuvette. Additionally, a small magnetic stir bar was inserted for sample stirring. The speed was adjusted to achieve light transmittance between 85% and 90% of red light and between 80% and 90% of blue light. The amount of powder in the cuvette was adjusted accordingly. Following indices were used for measurements:

Real refractive index – mannitol: 1.330
Real refractive index – trehalose: 1.652
Refractive index diethyl ether: 1.352
Imaginary index – mannitol: 10.0
Imaginary index – trehalose: 2.0

Imaginary indices were chosen experimentally to obtain smallest possible R parameter (here $R < 0.08$ at all measurements). The quality of these measurement is given by the $R$ parameter which decreases if the predicted scattering of the particle size distribution measurements fits with the detected scattering of the sample.[19] Measurements were executed on three different batches.

### 2.8. Scanning Electron Microscopy

A small amount of powder was placed on top of a stub covered with double-sided carbon tape. Before analysis, the stub was coated with carbon under vacuum for 40 s. The morphology of particles was examined by scanning electron microscopy (SEM) using a FEI Helios G3 UC (Thermo Fisher Scientific, Schwerte, Germany).

### 2.9. Residual Water Content

For trehalose and mannitol microparticles, ≈5 mg and 15 mg were weighed into a 2R vial, respectively. Three different batches were measured in triplicates, each. Also, a 1% water standard was prepared with ≈10 mg. After filling, a small piece of ceramic wool (Analytik Jena AG, Jena, Germany) was applied on top to avoid particle suction through the titrator. Vials were closed with a plastic stopper. Empty vials acting as blank values were treated accordingly. For coulometric measurements, an Aqua 40.00 Karl Fischer Titrator with corresponding software from Analytik Jena AG (Jena, Germany) was used. First the oven was heated to 100 °C, and the system was cleared of residual humidity by inserting an empty closed vial and activating the pump until a final drift of less than 8.0 µg $min^{-1}$ was reached. The specified drift was used and stop conditions were set to a total measurement time of 10 min or until the drift reached ≤2.0 µg $min^{-1}$ of the initial drift. Blank measurements were executed and automatically subtracted from standard and samples. Measurements were considered correct if the 1% water standard measurement resulted in a value between 0.9% and 1.1%.

### 2.10. Differential Scanning Calorimetry (DSC)

For calorimetric measurements, 3–5 mg of sample were weighed into a concavus pan and closed. The reference was an empty closed concavus pan. Reference and sample were inserted into the oven at a set point of 25 °C, and the oven was closed. Measurements were taken with a DSC 214 Polyma (Erich NETZSCH GmbH & Co. Holding KG, Selb, Germany) starting from −10 °C with a ramp of 8 °K $min^{-1}$ until temperature reached 160 °C for trehalose or 200 °C for mannitol formulations. Data were analyzed using the Proteus Analysis software.

### 2.11. X-Ray Powder Diffraction (XRPD)

For identification of crystalline and or amorphous structures XRPD was executed with a 3000 TT diffractometer (Seifert, Ahrensburg, Germany). Equipped with a copper anode with a voltage of 40 kV and a current of 30 mA, a wavelength of 0.154178 nm was used. The voltage of the scintillation detector was 1000 V. Samples placed on the copper sample holder were analyzed in the range of 5–40° 2-theta in steps of 0.05° 2-theta.

### 2.12. Aerodynamic Properties

For analysis of aerodynamic properties apparatus E of the European Pharmacopoeia was used from Copley Scientific (Nottingham, UK). The next generation impactor (NGI) was fitted with a pre-separator (PS) and an induction port (IP). The instrument was connected to a critical flow controller (TPK 2, ERWEKA GmbH, Langen, Germany) to ensure correct valve opening for a predetermined time to allow a total volume of 4 L air passing through the instrument for each measurement. Further on, the TPK was connected to a high performance vacuum pump (HVP 1000, ERWEKA GmbH) generating a flow rate which was set to 30 L $min^{-1}$ (volumetric L $min^{-1}$) by a TSI 4040 flowmeter (TSI Instruments Ltd., High Wycombe, UK). A stock of 0.167× Tris-EDTA (TE) solution was prepared by mixing 0.5 mL 100× TE with 299.5 mL HPW. Prior to each analysis, the pre-separator was filled with 10 mL of Heparin-TE solution (23.3 mg Heparin in 60 mL 0.167× TE) (HTE) and cups were coated with 10 µL of a solution containing 83% glycerin, 14% ethanol, and 3% Brij 35.[20] Cotton swabs pre wetted with coating solution were used to distribute the coating solution across the entire cup area. For analysis, 4 or 8 hydroxypropylmethylcellulose capsules were loaded with ≈45 mg of 5% or 10% w/v spray dried formulations, respectively. Each capsule was loaded into a Handihaler (Boehringer Ingelheim Pharma GmbH & Co. KG, Ingelheim, Germany) and activated by piercing. According to the manufacturer's manual, the capsules were discharged twice with an interval between the two actuations of 5 s. After discharging the content of capsules into the impactor, the IP was carefully taken off and closed with two rubber stoppers after 10 mL of HTE were inserted. Also, the PS was carefully removed and both openings were closed with plastic stoppers. Both, IP and PS, were shaken vertically and horizontally for 1 min. Finally, the NGI was disassembled and the small cups were filled with 2 mL HTE, whereas the greater cups were filled with 4 mL HTE. All cups were covered with a plastic lid to avoid solvent evaporation. The cups were placed on a shaker for 5–10 min, and the rotation speed was set in a fashion to avoid spilling but ensure complete dispersion of particles. Three aliquots of 100 µL from each stage including IP and PS were prepared for further analysis. The mass of siRNA

deposited on each stage was analyzed as described under 2.13 with an extended standard point line toward the lower limit. This experiment was carried out with three different batches. The mass median aerodynamic diameter (MMAD), geometric standard deviation (GSD), fine particle dose (FPD), and fine particle fraction (FPF) were calculated as described in the European Pharmacopoeia.[14b] "Fine particles" were considered all particles below 5 µm MMAD.

### 2.13. siRNA and PPP Quantification

Quantification assays were performed as described earlier.[9] In short, 50 mg for 5% and 100 mg for 10% matrix formulations, respectively, were transferred into a 2 mL volumetric flask and dissolved in HPW to release polyplexes. These solutions were used for the following assays:

#### *2.13.1. TNBS Assay*

An aliquot of 100 µL of each sample was taken and mixed with 0.088% w/v TNBS in 0.1 M borax. After an incubation time of 1 h, samples were analyzed with a quartz cuvette in a UV-1600PC spectrophotometer (VWR International GmbH, Darmstadt, Germany) at an absorbance of 405 nm. Results were compared with an equally treated standard dilution series (0.166–1.914 µg) where a corresponding amount of siRNA was added to avoid biases. Measurements were only considered for further analysis if an internal standard (iS), prepared as described in Section 2.3, showed a deviation of less than ± 10% compared to the theoretical amount.

#### *2.13.2. Heparin SYBR Gold Assay (HepSYBR)*

An aliquot of 60 µL of each sample was taken and diluted with HPW to 150 µL. To dissociate siRNA from polymer, 75 µL of 2.33 mg $mL^{-1}$ heparin solution in TE buffer was added and incubated for 2 h. After dilution with HPW to 450 µL, triplicates of 100 µL were pipetted into a black 96 well plate. A dilution series starting at 0.09 µg 100 $\mu L^{-1}$ was prepared and added in triplicates into the same 96 black well plate. To verify full dissociation of siRNA and polymer, an iS was prepared as described in Section 2.3, treated alike and analyzed in triplicates. A 4× SYBR gold solution in HPW was prepared for intercalation of double stranded RNA and 30 µL were added to each well with an 8-channel multi pipette. Fluorescence was measured at an excitation wavelength of 485/20 nm and an emission wavelength of 520/20 nm on a FLUOstar Omega multi-mode microplate reader (BMG LABTECH GmbH, Ortenberg, Germany). Measurements were considered for further analysis if iS showed a deviation of less than ± 10% compared to the theoretical amount.

### 2.14. Integrity test

To achieve a final gel loading amount of 150 ng siGFP per lane ($m(siGFP)_{lane}$), siRNA losses detected by HepSYBR were considered (recovery), and the following calculation was used to determine the amount of spray dried powder (m(NIM)):

$$m(NIM) = m(siRNA)lane * \frac{m\,(tsc)}{m(siRNA)_{sd}} * recovery \quad (2)$$

where m(tsc) is the total solid content of the spray dried powder and $m(siRNA)_{sd}$ is the initial amount of siRNA used for spray drying, i.e., 30 µg. Powder was weighed and reconstituted in 15 µL of HPW and 5 µL of Heparin (12 µg Heparin per 5 µL TE-buffer). After 30 minutes of incubation, 4 µL of the 6× loading dye was added and a 4–20% TBE gel (EC62252BOX, ThermoScientific, Germany) was loaded with 24 µL of each sample. For control, free siRNA and siRNA with heparin were loaded as well. The gel was run at a constant voltage of 200 V for up to 1 h in Tris-Borate-EDTA buffer (TBE) until lanes separated. Gels were taken off the chamber and placed in 20 mL of a 1× SYBRsafe solution for 30 min under 50 rpm shaking. Gels were analyzed using a ChemiDoc fluorescence detector (Bio-Rad Laboratories GmbH, Feldkirchen, Germany).

### 2.15. In Vitro Gene Silencing

For in vitro gene silencing assessment, a non-small cell lung cancer line H1299 (ATCC CRL-5803) stably expressing enhanced green fluorescence protein (GFP) was used. Cells were cultivated in RPMI-1640 supplemented with FBS (10%), P/S (1%) and G418 (0.4%) for selection at 37 °C with 5% $CO_2$. Cells were seeded into 24 well plates with a density of $2 \times 10^5$ cells per well and a total volume of 500 µL medium 24 h prior to the experiment. On the day of transfection, the medium was replaced with 400 µL fresh medium and 100 µL of siRNA polyplexes were applied to obtain a final concentration of $100 \times 10^{-9}$ M siGFP or siNC. As different spray dried formulations at different concentrations were tested and detected losses had to be taken into account, the amount of powder and hence of excipient had to be adjusted. Therefore, samples within the same group were treated to contain equal amounts of excipient for better comparability. After 72 h, medium was discarded, cells were washed with PBS, trypsinized and collected. After centrifugation at 400 rcf for 5 min, the supernatant was discarded and the cell pellet was resuspended in PBS. Samples were analyzed by flow cytometry (Attune Acoustic Focusing Cytometer, Life Technologies), and the median fluorescence intensity (MFI) was measured using 488 nm excitation and a 530/30 nm band pass emission filter set (BL-1H). Samples were run in triplicates for each batch, with each sample gated regarding cell morphology based on forward/sideward scattering for a set of 10 000 viable cells. Triplicates of each batch were summarized by generating the mean value.

### 2.16. GATA3 Silencing Ex Vivo in Primary $CD4^+$ Cells

Transferrin-PEI (Tf-PEI) polyplexes prepared with a 1:1 mixture of two different siRNA sequences against GATA3 (HS_GATA3_8–SI04212446, and HS_GATA3_9–SI04364101, Qiagen, Hilden, Germany) were prepared as previously described.[16] The formulation was previously characterized

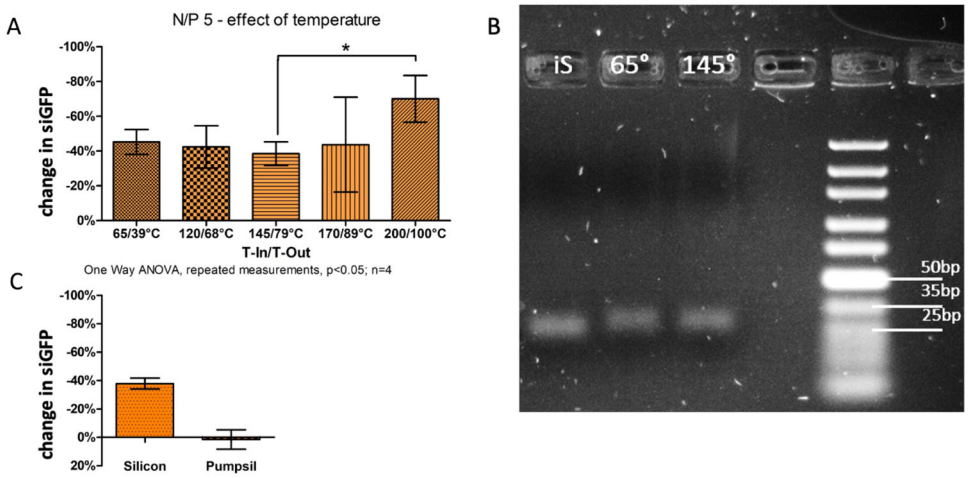


**Figure 1.** A) Quantification of siGFP after spray drying of polyplexes (N/P 5) at various T-In. B) Agarose gel of redispersed polyplexes after spray drying with indicated T-In in °C. siGFP was released from polyplexes upon incubation with heparin. Lane 1: internal standard (iS), Lane 2: powder spray dried at 65 °C T-In, Lane 3: powder spray dried at 145 °C T-In, Lane 5: low range DNA base pair ladder. C) Quantification of siGFP after pumping polyplexes through standard silicon tubing and Pumpsil tubing ($n = 3$).

regarding physicochemical characteristics, stability in presence of mucus and surfactant, and its ability to target T cells in the lung of mice.[16a] Here, Tf-PEI polyplexes were spray dried as described in Section 2.4 containing 1760 pmol 5 $mL^{-1}$ of 5% v/v trehalose or mannitol. The powder was analyzed in Sections 2.8, 2.11, and 2.12 for quality control, and to ensure exact amounts of siGATA3 for transfection.

Primary $CD4^+$ T cells were isolated from freshly obtained buffy coats (Bavarian Red Cross (BRK), Munich, Germany) as described before.[16] Ethics approval for the production of "Buffy Coats for Research Purposes" was obtained by the BRK according to German laws and the EU Guidelines 2002/98/EC, 2004/33/EC, and 2005/62/EC. Isolated $CD4^+$ T cells were cultured in RPMI medium supplemented with 10% FBS, 1% P/S, $10 \times 10^{-3}$ M HEPES, $1 \times 10^{-3}$ M sodium pyruvate and 4500 mg $L^{-1}$ glucose. For GATA3 silencing, $8 \times 10^6$ primary T cells were seeded in a 48 well plate containing 200 µL medium. Primary T cell activation was executed by using Dynabeads Human T-Activator CD3/CD28 (11131D, Life Technologies) following the supplier's protocol of mixing beads and cells 1:1. Spray dried powder formulations containing Tf-PEI and siGATA3 were redispersed in nuclease free water. Controls consisting of siGATA3 or siNC were prepared with Tf-PEI or LF. After two days of T cell activation, the cells were transfected with freshly prepared or redispersed with a final concentration of $100 \times 10^{-9}$ M siRNA. Cells were incubated for 48 h and after removal of Dynabeads and lysed with the PureLink RNA mini kit according to the manufacturer's protocol (12183025, Thermo Fisher Scientific). In short, cells were washed, lysed, and RNA was isolated with an additional DNase digestion step. Afterwards, cDNA was synthesized using the high capacity cDNA Synthesis kit (#4368814, Applied Biosystems). After obtaining cDNA, the solution was diluted 1:10 and a qRT-PCR was run with custom synthesized GATA3 forward and reverse primers (Thermo Fisher) and $\beta$-actin primers (Qiagen, Hilden, Germany) for normalization. Cycle thresholds were acquired by auto setting within the qPCRsoft software (Analytik Jena AG, Jena, Germany).

### 2.17. Statistics

Experimental data were checked for significant difference by the GraphPad Prism 5 software using either One Way or Two Way ANOVA repeated measurements, with either Bonferroni or Dunnetts post-hoc test with $p > 0.05$ considered not significant (ns), and * $p < 0.05$, ** $p < 0.01$, *** $p < 0.001$ considered significantly different.

## 3. Results and Discussion

### 3.1. Heat Evaluation and Integrity

Spray drying is the most straight-forward technique for preparing microparticles. However, heat is a central necessity which could have a tremendous effect on siRNA. Hence, we spray dried polyplexes in presence with trehalose (10% w/v) at various inlet temperatures (T-In). As shown in **Figure 1**, increasing T-In up to 170°/T-Out 89 °C had no significant effect on the quantity of siGFP. At T-In of 200 °C/T-Out 100 °C, a significant increase in siGFP loss was detected. As siRNA melts at around 90 °C and switches from the double stranded to the single stranded form, it was important to avoid heating the siRNA formulation to this temperature for extended periods of time. The product temperature reached during the spray drying process is determined as the outlet temperature (T-Out).[21] Hence, the temperature which affects the product is equal to T-Out and therefore crucial for stability and integrity. For T-In at 200 °C and a subsequent T-Out of 100 °C, melting of siRNA occurred despite the polymer-based nanoformulation and consequently resulted in higher susceptibility to degradation.[15c, 22] Such high temperatures can potentially also lead to polyplex dissociation and siRNA release from the polyplexes. Protection of siRNA against heat and shear forces might therefore be decreased which could explain the greater loss at such elevated temperatures. However, the loss of siRNA due to thermal degradation is restricted as the exposure time of polyplexes to these temperatures is extremely low. Also,

a large variation in siRNA recovery, reflected in a comparably great standard deviation, was observed for spray conditions at 170 °C T-In (89 °C T-Out). At T-Out (89 ± 1.5 °C), the melting temperature of siRNA was almost reached. Therefore, melting may have occurred, leading to greater siRNA losses. It was hence decided that the highest suitable temperatures for spray drying siRNA polyplexes was 145 °C T-In and a subsequent T-Out of 79 °C. Furthermore, we hypothesized that spray drying can also be successful without elevated losses at even higher T-In if the equipment is set up in a fashion that T-Out remains below 90 °C. This could be achieved for example by increasing the feed or aspirator rate when increasing T-In at the same time.[21]

As the siRNA quantification described here relies on intercalation of a fluorescent dye which does not reflect the nucleic acid integrity, the latter has to be confirmed separately. This was achieved via gel retardation assay with samples obtained at the lowest T-In and the highest acceptable T-In (145 °C). Figure 1B confirms the duplex length of about 25 bp for the internal standard as well as the spray dried samples obtained at both process parameters. Hence, siRNA integrity in the recovered material even at the highest applicable T-In was maintained.

Although T-In/T-Out was reduced to minimize siRNA losses and duplex integrity was confirmed, nucleic acid losses appeared still rather high with ≈40%. To further elucidate the reasons for these losses, the effect of pumping polyplex suspensions from the sample container into the spray dryer was investigated. To test this effect, a polyplex suspension was pumped through the silicon tubing connected to the spray dryer and was collected afterwards. Interestingly, quantification of siGFP after pumping with regular quality silicon tubing, which was used in the experiments described above, revealed losses of around 40% (Figure 1C). These losses correspond to detected losses of redispersed polyplexes after spray drying. We therefore inferred that the measured losses during spray drying (Figure 1A) are not solely linked to the spray drying process itself but rather to the pumping step and the used tubing material. We further hypothesized that the adsorption of siGFP is due to hydrophobic interactions which was previously shown for DNA. [12] Furthermore, we tested whether high quality silicon tubing would reduce siRNA adsorption. And indeed, siGFP losses were reduced to 0% in Pumpsil tubing (Figure 1C). One explanation for the different adsorption behavior of siRNA polyplexes on high versus regular quality silicon tubings might be abrasion which takes place in the latter tubing and results in cavities. These superficial changes lead to an increase and regeneration of surface area, and hence to an increase of possible interactions between siGFP and the tubing material. Therefore, low abrasion tubings such as Pumpsil seem advantageous for the processing of polyplexes. The detailed mechanism for adsorption however is not within the scope of this article and will be addressed in future work.

### 3.2. Nanoparticle Characteristics

Besides heat, spray drying exerts shear forces on nanoparticles and could disassemble polyplexes. Hence, DLS measurements were performed before and after spray drying to visualize any possible effects. Thus, microparticles were dissolved in HPW for nanoparticle redispersion to mimic impaction and matrix excipient dissolution in the lung. As demonstrated in **Figure 2**, Z-average values of freshly prepared and redispersed polyplexes do not differ from each other statistically. Also, differences in PDI were not observed. However, we recognized high PDI values which might be explained to some extent by sugar/sugar alcohol monomers. It was shown by Weinbuch et al. that monomers of sugar and sugar alcohol are visible in highly concentrated solutions.[23] And indeed, we accordingly detected monomers at around 1 nm which are not visible if polyplexes are prepared in HPW instead (Figure S5, Supporting Information). This hypothesis is underlined by the fact that with increasing amount of excipient the peak at 1 nm increases (Figure S5, Supporting Information). This phenomenon also explains the trend of higher PDI values at higher concentrated excipient solutions. Nonetheless, Z-averages and PDI did not differ significantly within one excipient group. However, trehalose formulated polyplexes showed higher PDI values than mannitol formulated polyplexes which might be again attributed to a higher monomer content. In summary, polyplex size and distribution were not affected by spray drying within each formulation.

Furthermore, to confirm integrity and hence the base pair length of siRNA in all formulations, a gel assay was executed. **Figure 3** shows that independent of the chosen formulation and T-In, siRNA was intact in all cases reflected by all bands being detected at the same base pair length. Bands with a smaller molecular weight, which would indicate degradation of siRNA, were not detected. Smears below the siRNA bands accompanying all spray dried samples are attributed to heparin as shown by similar effects in the sample containing free siRNA mixed with heparin but not in the sample containing free siRNA without heparin. Hence, we stated that the base pair length of siRNA was not influenced by spray drying.

However, Z-average, PDI and base pair length are considered qualitative approaches to determine successful spray drying whereas determination of siRNA and polymer content are quantitative and hence extremely relevant for correct dosing. Therefore, the content of siRNA was analyzed in redispersed particles, and considerable losses were found when polyplexes were spray dried in the presence of mannitol (**Figure 4**A). However, when polyplexes were spray dried with trehalose, no significant loss of siRNA was observed. Hence, statistically significant differences in regard to siRNA recovery after spray drying between the two different matrix formulations at both spray drying temperatures were observed. As analyzed by two-way ANOVA, the choice of excipient was identified as the source of variation accounting for 58.6% of total variation and a p-value of 0.0013 indicating a highly significant effect. Similarly, polymer quantification resulted in no difference in recovery after spray drying when polyplexes were formulated with trehalose but showed losses of ≈53% and 65% when formulated with 5% mannitol or 10% mannitol, respectively. Here, no statistical differences between both temperatures and concentrations were detected within each excipient group. However, all mannitol formulations showed significantly higher losses in polymer than their trehalose formulated counterparts. Hence, mannitol formulations were outperformed by their trehalose formulated counterpart in respect to siRNA and polymer recoveries. This observation might be explained by the fact that trehalose formulations form amorphous particles whereas mannitol crystallizes upon spray drying as discussed below. It

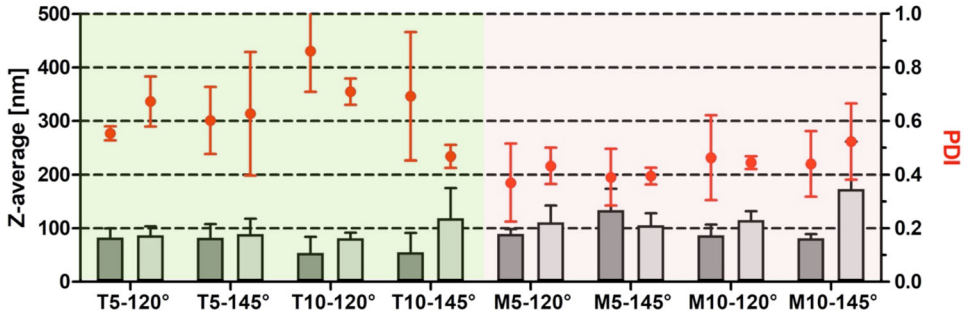


**Figure 2.** DLS measurements of freshly prepared (dark gray bars) and redispersed (light gray bars) spray dried PPP/siRNA polyplexes at indicated temperatures in °C with an N/P of 10 in presence of either trehalose (T) or mannitol (M) with an excipient concentration of either 5% or 10% related to the spray dried suspension. PDI is indicated by red circles. (each condition $n = 3$).

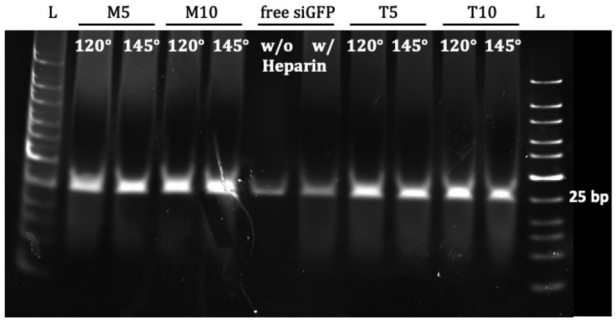


**Figure 3.** Agarose gel of redispersed polyplexes after spray drying with mannitol or trehalose at indicated T-In in °C. siGFP was released from polyplexes upon incubation with heparin. M5/T5: 5% w/v mannitol/trehalose formulation of siGFP/PPP (N/P 10); spray dried. M10/T10: 10% w/v mannitol/trehalose formulation of siGFP/PPP; spray dried. L: Ultra low range base pair ladder.

was shown previously that amorphous structures can stabilize biomacromolecules during drying.[24] Although this effect was not reported for polyplexes, it is not surprising that trehalose stabilizes polyplexes also. One explanation for this phenomenon is the water replacement theory.[25] During desiccation, trehalose stabilizes the structure of the entrapped molecules by forming hydrogen bonds and maintaining the three-dimensional structure. Also, higher residual moisture content of trehalose formulations as discussed below might add to this fact enabling greater stabilization by forming additional hydrogen bonds and acting as a plasticizer. In contrast, crystalline mannitol was shown to inefficiently stabilize biopharmaceuticals and might not protect the formulation from a drying-stress induced strand dissociation or potential degradation of the double stranded siRNA.[26] The dissociation of double stranded siRNA due to temperatures close to the melting point could have led to the decreased detection of siRNA with the intercalation based fluorescence quantification as described above which does not detect single stranded short RNA. This proposed mechanism is reinforced by the fact that detection of smaller double stranded nucleic acid strains, which would be found if double strand breaks had occurred, was not detected in the gel shift experiment (Figure 3). While the sensitivity for NOVEX gels is reported to be 60 pg for double-stranded DNA after SYBR Green staining,[27] no specific sensitivity is reported for SYBRSafe staining of double-stranded RNA. However, it is assumed that a loss of 0.1% (i.e., 150 pg out of the loaded 150 ng) should have become visible. Further electrophoresis-based methods such as capillary electrophoresis with the Agilent BioAnalyzer, for example, or HPLC-based techniques were therefore not performed.

### 3.3. Microparticle Characteristics

Pulmonary delivery via dry powder formulation requires low residual moisture in order to avoid aggregation processes. Although it was discussed above that residual moisture may act as a plasticizer stabilizing polyplexes during the spray drying process, it could nonetheless cause microparticle aggregation and

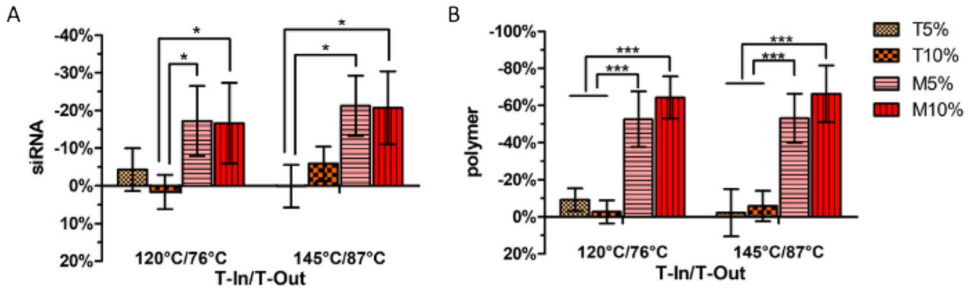


**Figure 4.** Quantification of A) siRNA (siGFP) and B) polymer (PPP) after spray drying at two different temperatures with two different excipients at two different concentrations. (each condition $n = 4$) M5/T5: 5% w/v mannitol/trehalose formulation of siGFP/PPP (N/P 10); spray dried. M10/T10: 10% w/v mannitol/trehalose formulation of siGFP/PPP (N/P 10); spray dried.

**Table 1.** Residual moisture of siGFP/PPP polyplexes (N/P 10) spray dried at 5% or 10% w/v with indicated excipient at 120 or 145 °C T-In.

| Concentration–temperature | Residual moisture [%] Trehalose formulations | Residual moisture [%] Mannitol formulations |
|---|---|---|
| **5%–120 °C** | 4.53 ± 0.20 | 0.40 ± 0.03 |
| **5%–145 °C** | 3.85 ± 0.05 | 0.27 ± 0.04 |
| **10%–120 °C** | 4.61 ± 0.17 | 0.26 ± 0.02 |
| **10%–145 °C** | 3.82 ± 0.04 | 0.19 ± 0.03 |

could be a source of microbiological instability and RNase contamination. Therefore, the water content of all formulations was measured by Karl Fischer titration. As reflected in **Table 1**, trehalose formulations exhibited between 4.6% and 3.8% whereas mannitol formulations showed between 0.4% and 0.2% residual moisture. These results were expected and are in line with results from the literature.[28]

Trehalose commonly solidifies upon spray drying in an amorphous state which was confirmed via DSC (**Figure 5**). In addition with the hygroscopic nature of trehalose, the reason for the formation of amorphous structures is the fast drying step which does not provide sufficient time for trehalose molecules to arrange within an ordered structure with subsequent crystal nucleation and growth.[29] All of the trehalose formulations showed glass transitions at temperatures between 38 and 53 °C corresponding to their residual moisture content (Table 1). This temperature ($T_g$) is important for stability predictions during storage as amorphous solid forms are thermodynamically unstable and tend to crystallize if stored close to or above $T_g$.[30] As discussed above in the context of siRNA recovery after spray drying, the amorphous state of the formulation is favorable for polyplex preservation. Hence, for storing these products at room

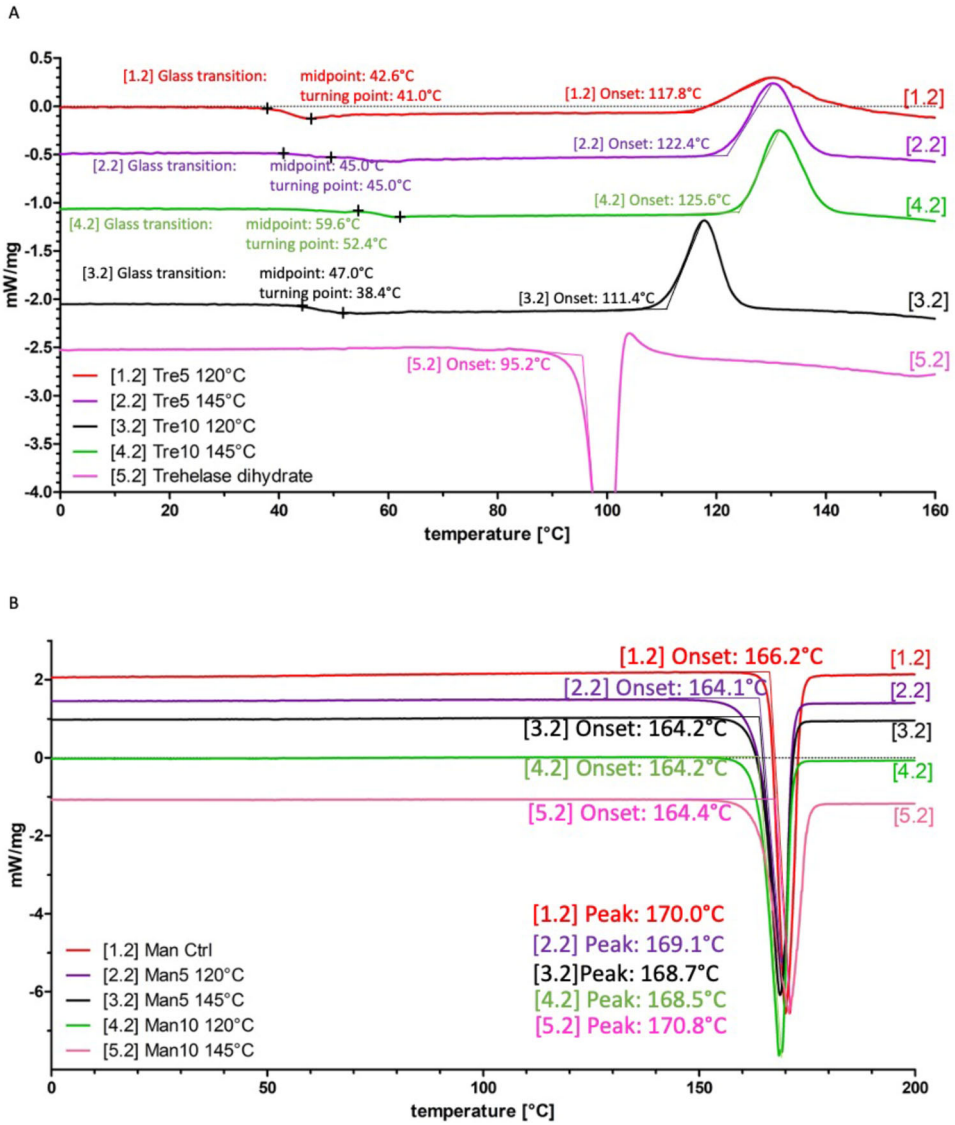


**Figure 5.** DSC measurements of Trehalose and Mannitol formulations: A) 1.2) T5–120 °C, 2.2) T5–145 °C, 3.2) T10–120 °C 4.2) T10–145 °C, 5.2) trehalose dihydrate. B) 1.2) crystalline mannitol 2.2) T5–120 °C, 3.2) T5–145 °C, 4.2) T10–120 °C, 5.2) T10–145 °C.

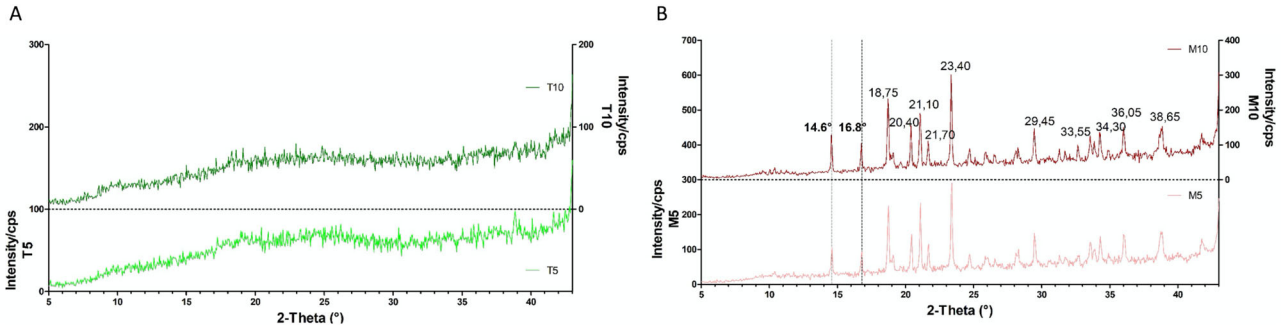


**Figure 6.** XRPD measurements of A) Trehalose and B) Mannitol formulations spray dried at 145 °C per 79 °C T-In per T-Out.

temperature or in the fridge for a longer period of time, high $T_g$ values are necessary. The $T_g$, however, is closely linked to the water content: the higher the residual moisture the lower $T_g$.[31] Also, with a lower residual moisture content degradation processes are less likely to occur.[31] It is therefore of great interest to further decrease the amount of residual moisture in trehalose formulations to avoid nucleation and degradation processes over time and in order to maintain the amorphous state of the formulation. While the impact of storage upon polyplex quality (size, PDI) and quantity has not yet been investigated, these aspects are currently under investigation in a greater scheme of optimizing formulation and process parameters. To confirm the amorphous state of trehalose, formulations were also tested by XRPD and typical amorphous halos were detected (**Figure 6**A). On the other hand, spray dried mannitol formulations exhibited the same temperature profile as the crystalline starting substance with a melting peak at 170 °C as investigated by DSC (Figure 5B). This finding indicates a crystalline form of mannitol. For distinct differentiation between the mannitol polymorphs which could possibly appear, XRPD was performed on formulations prepared at T-In of 145 °C. For both tested mannitol formulations, peaks at 14.6° and 16.8° 2-theta were detected which are both linked to the $\beta$ form of mannitol (Figure 6B).[29,32] Peaks specific for the $\alpha$ or $\delta$ form were not detected, indicating that after spray drying $\beta$ mannitol is the predominant polymorph. Although the drying time of spray dried formulations is very short and could have resulted in an amorphous state as obtained with trehalose, mannitol is less hygroscopic and less soluble. These characteristics lead to quicker drying of mannitol solutions and crystallization during spray drying. As the residual moisture content was lower for formulations prepared at higher temperatures and no significant differences in nanoparticle characteristics were found between formulations prepared at the two different temperatures, all subsequent experiments were conducted with formulations produced at a T-In of 145 °C.

To get a first understanding of microparticle size characteristics, static light scattering was performed in diethyl ether in which neither mannitol nor trehalose is soluble. As visualized in **Figure 7**, formulations differ from each other depending on the nature of excipient they are made of: both mannitol formulations show significantly lower values in the 10, 50, and 90 percentiles compared to the trehalose formulations (data not shown). Mannitol formulations exhibited geometric median sizes of around 7 and 8 µm for 5% and 10% formulations, respectively,

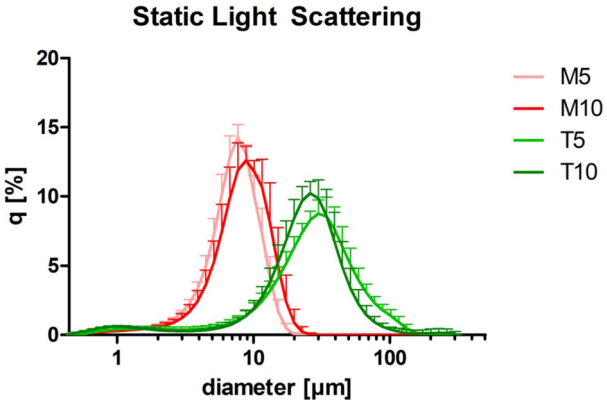


**Figure 7.** Particle size distribution of microparticles made of spray dried siGFP/PPP polyplexes as measured by SLS of M5–145 °C, M10–145 °C, T5–145 °C, T10–145 °C.

**Table 2.** Microparticle characteristics of polyplexes spray dried at 5% or 10% w/v with indicated excipient at 145 °C T-In. T: Trehalose; M: Mannitol; MMAD: Mass Median Aerodynamic Diameter; GSD: Geometric Standard Deviation; FPF: Fine Particle Fraction; FPD: Fine Particle Dose.

| | Geometric median diameter [µm] | MMAD [µm] | GSD [µm] | FPF [%] | FPD [µg] |
|---|---|---|---|---|---|
| **T5–145 °C** | 24.13 ± 1.47 | 4.65 ± 0.14 | 1.88 ± 0.07 | 14.0 ± 2.4 | 0.15 ± 0.09 |
| **T10–145 °C** | 24.02 ± 1.85 | 5.19 ± 0.47 | 1.95 ± 0.04 | 18.3 ± 5.0 | 0.11 ± 0.03 |
| **M5–145 °C** | 6.77 ± 0.35 | 4.77 ± 0.15 | 1.94 ± 0.03 | 32.3 ± 5.3 | 0.54 ± 0.05 |
| **M10–145 °C** | 8.02 ± 1.11 | 5.50 ± 0.29 | 1.97 ± 0.06 | 22.5 ± 2.4 | 0.21 ± 0.07 |

whereas trehalose formulations showed sizes of around 24 µm (**Table 2**).

This can be explained by the fact, that amorphous trehalose particles with higher residual moisture show a tendency towards particle fusion through water bridges.[33] Hence, although in fact particles were produced with similar diameters as in the mannitol formulations, as confirmed by SEM (**Figure 8**), these particles aggregate and may form greater secondary particles. This aggregation can be appreciated in the SEM micrographs (Figure 8). Whereas recordings of mannitol particles confirm the findings of SLS measurements, trehalose particles show much smaller geometric diameters. However, aggregation through water bridges can be observed as indicated by white arrows. Again, reductions

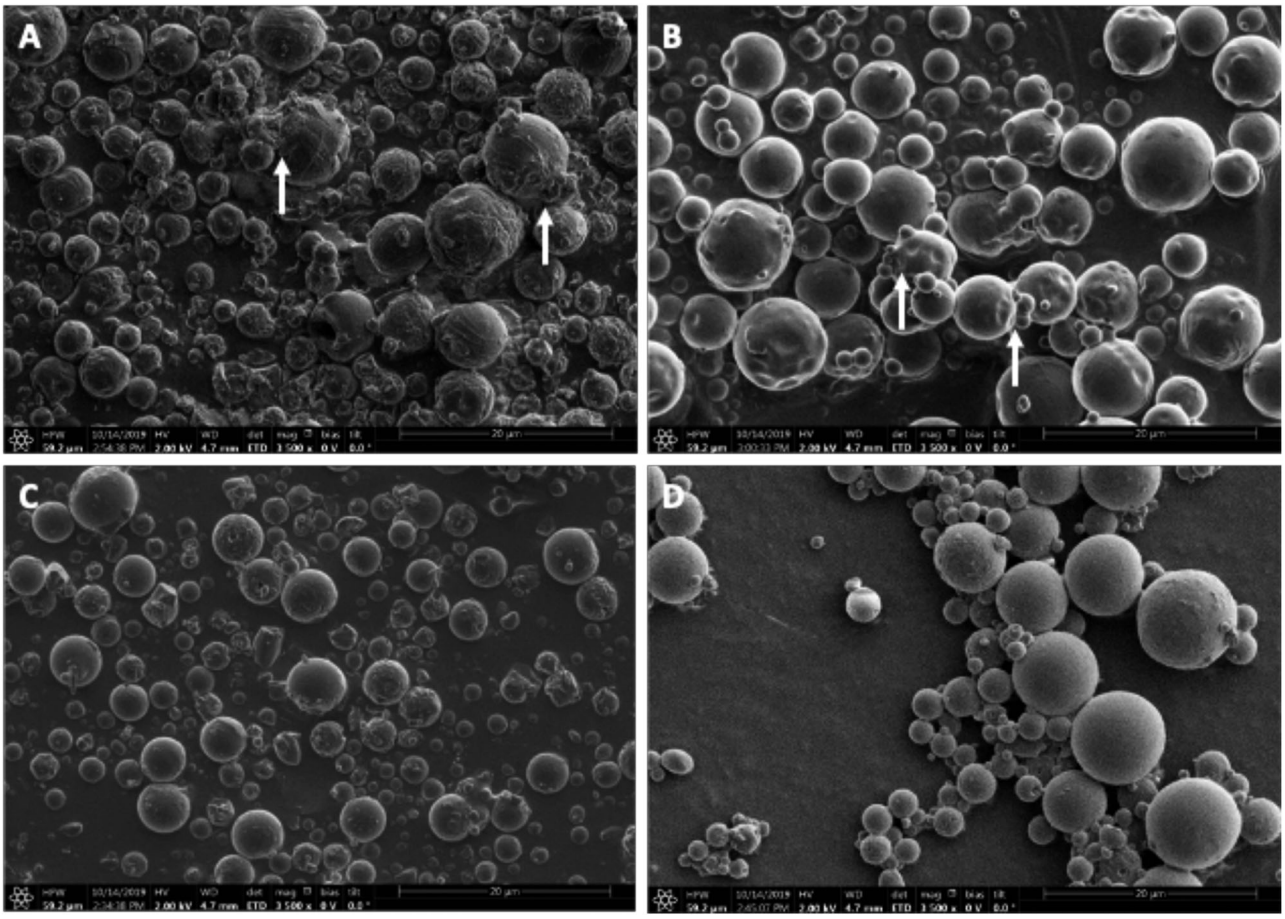


**Figure 8.** SEM pictures of A) T5–145 °C, B) T10–145 °C, C) M5–145 °C, D) M10–145°C. White arrows mark water bridges between single trehalose particles.

in the water content of trehalose microparticles could considerably reduce this effect. Concerning the surface of the particles, mannitol formulations in general exhibited a very smooth round structure. Trehalose particles also showed smooth surfaces when formulated at 10%, whereas 5% formulations indicated a somewhat roughened surface.

For pulmonary delivery, aerodynamic sizes between 1 and 5 µm are crucial for successful delivery to the alveolar space as discussed above. Although geometric median sizes were greater than 5 µm, the aerodynamic diameter also depends on the particle density and porosity and might therefore be lower as the geometric diameter.[34] In fact, measurements of impacted siRNA in the NGI revealed MMAD values close to or below 5 µm for trehalose and mannitol formulations, indicating successful lung delivery. Also, calculation of GSD suggests a particle distribution which can be considered for pulmonary application, particularly for bronchial diseases such as asthma or prophylaxis of respiratory virus infections. The FPF is considered the percentage of drug that was delivered in particles below 5 µm compared to the overall impacted drug on all stages of the NGI. The higher the FPF, the more drug could potentially be delivered to the alveolar space for potential systemic availability. Accordingly, fine particle fractions with 14–18% for both trehalose and 23–32% for both mannitol formulations, respectively, are considered very good. While only small amounts of particles collected in the NGI were below 5 µm and could potentially reach bronchioles and alveoli, asthma is a bronchial disease, and deposition in the larger airways can also be achieved with particles larger than 5 µm MMAD. However, to optimize the deposited dose and decrease side potential side effects, decreases in MMAD would be favorable. Compared to the FPF, the FPD is considered the dose of drug in µg which was actually delivered in particles with less than 5 µm MMAD. It is therefore not a ratio but an exact dose calculated based on the aerodynamic behavior of the powder. Here, FPD differed between mannitol and trehalose formulations: whereas mannitol formulations could potentially deliver more than 0.5 µg, only less than 0.2 µg of siRNA could currently be delivered to the deep lung by trehalose formulations described above. Although the FPFs in trehalose formulated polyplexes were much smaller, this finding cannot solely explain the discrepancy in FPD. To explain this phenomenon, it has to be taken into account that for FPF calculations only the deposited amount of drug inside the NGI is considered. Depositions in the pre-separator, induction port or even in the Handihaler device itself are not considered. And indeed, a large amount of powder was found on the inner walls of the application device's capsule rack which unfortunately was not quantified. This finding was noticed only for trehalose and not for mannitol formulations. The

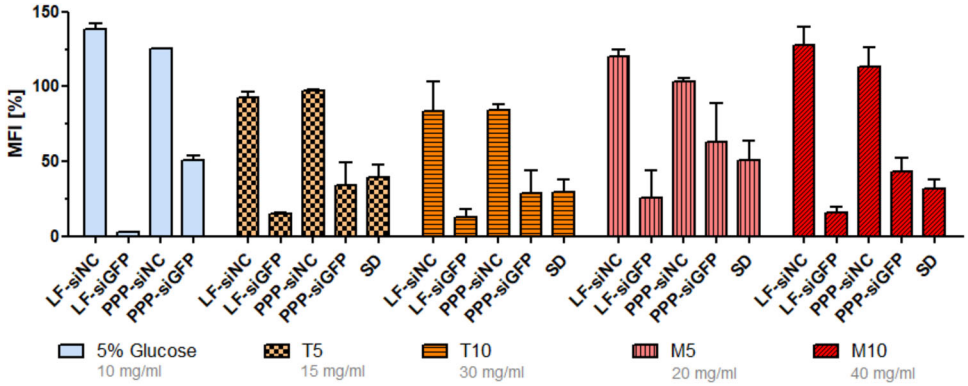


**Figure 9.** In vitro knockdown of GFP within a H1299 cell line stably expressing eGFP. Within each group, samples contain the same amount of excipient as indicated by the legend. LF: Lipofectamine, PPP: (mPEG-b-PCL)-g-PEI block copolymer, siNC: negative control siRNA, siGFP: siRNA sequence against eGFP, SD: spray dried polyplexes consisting of PPP and siGFP at 5% (w/v) total solid content at 145 °C T-In. Polyplexes were prepared at N/P 10. $n = 4$.

most reasonable explanation for this observation might be the amorphous structure of the powder and the higher residual moisture of trehalose formulations. After the release of powder from the capsule through the vacuum and the thus generated centrifugal forces, particles are forced to leave the Handihaler by following the airstream. Smaller and hence lighter particles can follow the airstream directly, whereas a great portion of particles which might be aggregated will follow the airstream only after impacting on and bouncing off the capsule rack's inner wall, thereby possibly disaggregating. However, due to the high residual water content and the subsequent plasticity of trehalose particles, a large amount of powder could adhere to the wall remaining within the device. This explains why suitable values were calculated for MMAD and GSD and FPF based on the amount of drug deposited inside the NGI from the trehalose formulations. Mannitol powders, on the other hand, were not detected in the capsule rack and hence are suggested to be successfully introduced into the NGI without further losses.

From the overall assessment of the microparticle properties, we therefore conclude that crystalline structures outperform amorphous substances regarding aerodynamic properties even if the amorphous state seemed favorable with regard to polyplex stability.

### 3.4. In Vitro Performance

For siRNA delivery it is fundamental to maintain the molecule's bioactivity. Prior to following experiments, the cytotoxicity for PPP in combination with or without siRNA was evaluated in MTT assays (Figure S6). Both polyplexes and polymer only did not cause any reduction in metabolic effect in the tested N/P range (N/P 6–20). Hence, spray dried powder was reconstituted, and enhanced green fluorescence protein (eGFP) expressing H1299 cells were transfected with redispersed polyplexes. Lipofectamine (LF) is a standard in vitro transfecting agent and is used as a positive control.[35] It is used to show the maximum possible gene silencing. In all cases siRNA was active as the expression of GFP was significantly decreased (**Figure 9**). Lipofectamine/siGFP complexes used in the standard in vitro formulation with 5% glucose showed the highest downregulation observed in all five groups which is >95% in relative reduction (compared to siNC/LF containing a negative control siRNA sequence). Interestingly, Lipofectamine complexes formulated with trehalose or mannitol with the respective concentration of excipient although successful in downregulation, only showed a relative reduction between 70% and 80%. One possible mechanism for this discrepancy might be explained by the fact that transfection is a process which is energy consuming and factors which provide energy to cells such as glucose are therefore favorable.[36] Exchanging glucose for trehalose or mannitol might therefore lower this positive effect and cells might take up particles less efficiently than in the glucose reference group. Whether this effect or the viscosity of the matrix solutions used here causes the decreased transfection remains unclear and is part of future research.

In previous studies polyplexes made of PPP and siRNA already showed knockdown efficiencies of ≈50% in vitro[37] and even >70% in vivo in the lung where Lipofectamine complexes are not stable and too toxic.[8a] Hence, it is of great importance to retain transfection ability and efficiency during spray drying for in vitro experiments and follow up studies in vivo. As demonstrated in Figure 9, polyplexes formed of siGFP and PPP performed better than their negative control formulations (siNC/PPP). Importantly, all spray dried polyplexes (SD) performed at least as well as their freshly prepared counterparts. This effect is independent of the excipient's nature and its concentration.

### 3.5. Ex Vivo Performance

After confirming bioactivity in vitro, the knowledge obtained in this study with siGFP/PPP polyplexes was transferred toward a clinically more relevant model in which the T-helper type 2 (Th2) transcription factor GATA binding protein 3 (GATA3) was attempted to be downregulated in primary human $CD4^+$ T cells. In severe uncontrolled asthma, Th2 cells play a crucial role in the activation of downstream effects which orchestrate the full manifestation of asthma which is caused by upregulated expression of GATA3.[38] Downregulation of such overexpressed proteins could lead to a significant improvement and thus benefit in therapy and administration frequency as shown for other siRNA based

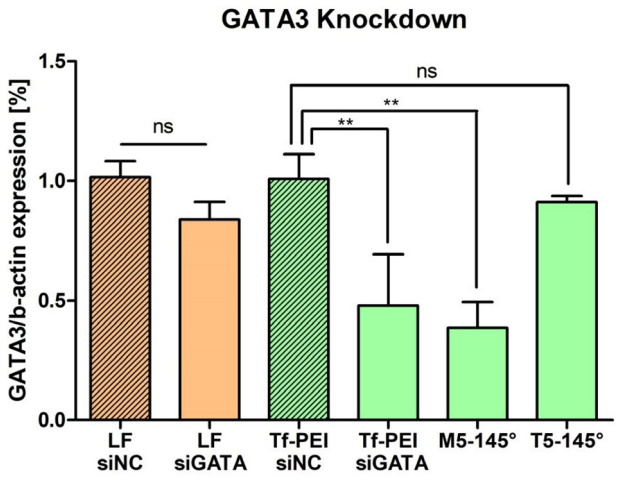


**Figure 10.** Ex vivo knockdown of GATA3 within primary CD4+ T cells; LF: Lipofectamine, Tf-PEI: Transferrin conjugated PEI, siNC: negative control siRNA, siGATA: siRNA sequence against GATA3, M5–145° per T5–145°: spray dried polyplexes of Tf-PEI and siGATA3 (N/P 10) at 145 °C T-In with 5% Mannitol or 5% Trehalose.

therapies.[39] Therefore, our group has optimized a delivery system for T cell transfection of siRNA, namely transferrin-coupled PEI (Tf-PEI), which has been characterized and described regarding physicochemical characteristics, stability in mucus and surfactant, toxicity in vitro and in vivo, and regarding T cell targeting in the lung and gene silencing.[16]

Here, siGATA3/Tf-PEI polyplexes were spray dried and characterized regarding residual moisture (Table S1, Supporting Information), aerodynamic properties (Table S2, Supporting Information), and siRNA losses (Figure S7). It was observed that the residual moisture did not depend as much on the polyplex system used as on the excipient, that aerodynamic properties were strongly affected by the residual moisture content, and that siRNA loss neither depends on the siRNA sequence nor on the polymer used for nanoformulation. While the siRNA losses and residual moisture reflected the trends observed for siRNA/PPP polyplex formulations, the slightly decreased residual moisture in the siRNA/Tf-PEI formulations containing trehalose increased the FPF for the formulation.

For the ex vivo transfection experiments, siRNA losses were taken into account, and cells transfected with freshly prepared or redispersed polyplexes. After two days of incubation, RNA was isolated from the transfected T cells, the amount of GATA3 mRNA was analyzed and normalized to $\beta$-actin. As expected, Lipofectamine showed no significant difference between the negative control siRNA and siGATA3 (**Figure 10**). Freshly prepared polyplexes consisting of Tf-PEI and siGATA3 however, mediated a significant reduction in the expression of GATA3, and most of all polyplexes of Tf-PEI and siGATA3 which were spray dried with 5% mannitol (M5–145 °C) showed identical effects. Importantly, the gene silencing efficacy of M5–145 °C did not differ significantly from that of freshly prepared siGATA3 containing polyplexes confirming retained bioactivity and transfection efficiency. Polyplexes spray dried with 5% trehalose, however, showed no transfection at all. This result was surprising as it was expected that amorphous substances such as trehalose would stabilize transferrin, a 79 kDa protein, to a greater extent than the crystalline mannitol, especially because the latter excipient is known to induce protein aggregation upon spray drying.[40] However, here, mannitol formulations stabilized transferrin sufficiently and allowed successful transfection. One plausible reason for the lack of gene silencing of the trehalose formulation might be redispersion problems in rather small volumes used for transfection considering their aggregation tendency shown in Figure 8. Successful stabilization of transferrin in the mannitol formulations could potentially be achieved by PEI in the polyplexes. PEI participates in the formation of polyplexes but could also interact within transferrin directly. And indeed, as was shown, PEI is able to physically crosslink a protein and increase its stability during stresses induced by pH shifts and stirring.[41] This could explain the maintained stability and conformation of Tf enabling recognition of Tf-receptors of T cells with the Tf decorated polyplexes. Further research will focus on the formation of protein aggregates, the secondary structure and binding kinetics of Tf when spray dried alone, in mixture with PEI and as a Tf-PEI conjugate in either mannitol or trehalose for a better understanding of the processes underlying these findings.

## 4. Conclusions and Outlook

In summary, we showed that spray drying above T-Out of 90 °C results in significant changes in the quantity of siRNA recovered after spray drying. Spray drying at temperatures below 90 °C showed no significant differences in respect to recovered quantity and base pair length. Furthermore, we were able to show that the tubing material can have a tremendous effect on the preparation and processing of spray dried polyplexes as interactions between the tubing material and siRNA may occur.

We demonstrated that spray drying did not affect polyplex size and PDI independent of the different excipients and their concentration used in this study. This was also shown for siRNA integrity. Quantitative analysis revealed significant losses of siGFP and PPP after spray drying when formulated with mannitol, a representative for crystalline substances. However, no changes regarding the recovery of both polyplex components were observed when spray dried with trehalose, the typical matrix used for amorphous microparticles. Therefore, we hypothesize that for nanoparticle properties amorphous substances are crucial to minimize losses through processing.

Concerning microparticle characteristics, mannitol formulations significantly outperformed trehalose formulations with regard to aerodynamic properties. Due to crystalline structure and subsequently lower residual moisture, mannitol particles exhibited smaller geometric median sizes and showed favorable aerodynamic characteristics.

For in vitro analysis, both formulations showed efficient downregulation of GFP in an eGFP expressing cell line indicating preserved bioactivity with all tested formulations. These findings were translated toward ex vivo gene silencing in primary $CD4^+$ T cells which play a central role in the pathogenesis of inflammatory diseases such as asthma where upregulation of the Th2 transcription factor GATA3 can be observed. We demonstrated that spray drying of polyplexes had no negative effect on the efficiency when formulated with mannitol, and successful transfection of primary T cells ex vivo was achieved with the spray dried

mannitol formulation for dry powder inhalation as reflected by efficient and sequence specific GATA3 silencing.

Since combining beneficial properties of both crystalline and amorphous particles for stabilization through the amorphous matrix and optimal microparticle characteristics through the crystalline material did not further improve nanoparticle and aerodynamic properties (data not shown), we are currently optimizing the spray drying process to include a secondary drying step which is expected to decrease the residual moisture content of trehalose formulations and possibly improve microparticle aerodynamic characteristics without lowering nanoparticle stability. Furthermore, studies will be carried out where spray drying will be performed at higher airflow to produce smaller particles and improve aerodynamic properties.

## Supporting Information

Supporting Information is available from the Wiley Online Library or from the author.

## Acknowledgements

T.W.M.K. and C.Z. contributed equally. This project was funded by the European Research Council (ERC) under the European Union's Horizon 2020 research and innovation program (Grant agreement No. ERC-2014-StG637830). The authors like to thank Dr. Mathias Keil for the NGI and Dr. Sibylle Welzhofer (Actarmo Medical GmbH) for NGI training. They also like to acknowledge Christian Minke for his work with the SEM and Watson Marlow for the kind supply of Pumpsil tubing. The authors would like to acknowledge the WACKER-Chair of Macromolecular Chemistry (Technical University Munich) for help with polymer synthesis and analysis.

Open access funding enabled and organized by Projekt DEAL.

## Conflict of Interest

The authors declare no conflict of interest.

## Data Availability Statement

Research data are not shared.

## Keywords

asthma, dry powder, inhalation, short interfering RNA (siRNA), spray drying

Received: March 15, 2021
Revised: April 10, 2021
Published online:

[1] S. Weber, A. Zimmer, J. Pardeike, *Eur. J. Pharm. Biopharm.* **2014**, *86*, 7.
[2] A. Ray, A. Mandal, A. K. Mitra, *Recent Pat. Drug Delivery Formulation* **2015**, *9*, 225.
[3] G. K. Crompton, *J. Aerosol Med.* **1991**, *4*, 151.
[4] P. Hematti, E. G. Schmuck, J. A. Kink, A. N. Raval, US Patent US20180282698A1 **2018**.
[5] S. Ambike, C. Cheng, S. Afridi, M. Feuerherd, P. Hagen, V. Grass, O. Merkel, A. Pichlmair, C. Ko, T. Michler, *researchsquare.com* **2020**.
[6] H. J. Kim, A. Kim, K. Miyata, K. Kataoka, *Adv. Drug Delivery Rev.* **2016**, *104*, 61.
[7] a) S. S. Titze-de-Almeida, P. R. P. Brandao, I. Faber, R. Titze-de-Almeida, *Mol. Diagn. Ther.* **2020**, *24*, 49, DOI: 10.1007/s40291-019-00434-w; b) P. de Paula Brandão, S. Titze-de-Almeida, R. Titze-de-Almeida, *Mol. Diagn. Ther.* **2020**, 49.
[8] a) D. P. Feldmann, Y. Xie, S. K. Jones, D. Yu, A. Moszczynska, O. M. Merkel, *Nanotechnology* **2017**, *28*, 224001; b) S. K. Jones, V. Lizzio, O. M. Merkel, *Biomacromolecules* **2016**, *17*, 76; c) T. Endres, M. Zheng, M. Beck-Broichsitter, T. Kissel, *Int. J. Pharm.* **2012**, *428*, 121.
[9] T. W. M. Keil, D. P. Feldmann, G. Costabile, Q. Zhong, S. da Rocha, O. M. Merkel, *Eur. J. Pharm. Biopharm.* **2019**, *143*, 61, DOI: 10.1016/j.ejpb.2019.08.012.
[10] K. Cal, K. Sollohub, *J. Pharm. Sci.* **2010**, *99*, 575.
[11] T. Okuda, M. Morishita, K. Mizutani, A. Shibayama, M. Okazaki, H. Okamoto, *J. Controlled Release* **2018**, *279*, 99.
[12] M. Cardenas, A. Braem, T. Nylander, B. Lindman, *Langmuir* **2003**, *19*, 7712.
[13] a) J. Horn, J. Schanda, W. Friess, *Eur. J. Pharm. Biopharm.* **2018**, *127*, 342; b) M. T. Cicerone, M. J. Pikal, K. K. Qian, *Adv. Drug Delivery Rev.* **2015**, *93*, 14.
[14] a) United-States-Pharmacopeial-Convention, 601 Aerosols, Nasal Sprays, Metered-Dose Inhalers, and Dry Powder Inhalers, USP 35 2012, 232; b) European-Pharmacopoeia-Commission, 2.9.18 Preparations for Inhalation, Ph. Eur. 9.0 2017, 440.
[15] a) W. Liang, M. Y. Chow, P. N. Lau, Q. T. Zhou, P. C. Kwok, G. P. Leung, A. J. Mason, H. K. Chan, L. L. Poon, J. K. Lam, *Mol. Pharmaceutics* **2015**, *12*, 910; b) W. L. Liang, M. Y. T. Chow, S. F. Chow, H. K. Chan, P. C. L. Kwok, J. K. W. Lam, *Int. J. Pharm.* **2018**, *552*, 67; c) J. Wu, L. Wu, F. Wan, J. Rantanen, D. Cun, M. Yang, *Int. J. Pharm.* **2019**, *566*, 32; d) J. Schulze, S. Kuhn, S. Hendrikx, M. Schulz-Siegmund, T. Polte, A. Aigner, *Small* **2018**, *14*, 1701810.
[16] a) Y. Xie, N. H. Kim, V. Nadithe, D. Schalk, A. Thakur, A. Kilic, L. G. Lum, D. J. Bassett, O. M. Merkel, *J. Controlled Release* **2016**, *229*, 120; b) R. Kandil, Y. Xie, R. Heermann, L. Isert, K. Jung, A. Mehta, O. M. Merkel, *Adv. Ther. (Weinheim, Ger.)* **2019**, *2*, 1900047.
[17] L. Liu, M. Zheng, D. Librizzi, T. Renette, O. M. Merkel, T. Kissel, *Mol. Pharmaceutics* **2015**, *13*, 134.
[18] Y. Liu, J. Nguyen, T. Steele, O. Merkel, T. Kissel, *Polymer* **2009**, *50*, 3895.
[19] HORIBA, https://www.horiba.com/fileadmin/uploads/Scientific/Documents/PSA/TN153.pdf 4.
[20] S. Claus, C. Weiler, J. Schiewe, W. Friess, *Pharm. Res.* **2013**, *30*, 1698.
[21] Büchi-Labortechnik-AG, https://static1.buchi.com/sites/default/files/downloads/Set_3_Training_Papers_Spray_Drying_en_01.pdf?996b2db24007502bd69c913b675467cfc63880ba 1997–2002.
[22] M. Terrazas, E. T. Kool, *Nucleic Acids Res.* **2009**, *37*, 346.
[23] D. Weinbuch, J. K. Cheung, J. Ketelaars, V. Filipe, A. Hawe, J. den Engelsman, W. Jiskoot, *Pharm. Res.* **2015**, *32*, 2419.
[24] a) N. K. Jain, I. Roy, *Protein Sci.* **2009**, *18*, 24; b) I. Vollrath, W. Friess, A. Freitag, A. Hawe, G. Winter, *Int. J. Pharm.* **2019**, *558*, 18; c) J. H. Gitter, R. Geidobler, I. Presser, G. Winter, *J. Pharm. Sci.* **2018**, *107*, 2748; d) J. H. Crowe, L. M. Crowe, D. Chapman, *Science* **1984**, *223*, 701.
[25] J. H. Crowe, F. A. Hoekstra, L. M. Crowe, *Annu. Rev. Physiol.* **1992**, *54*, 579.
[26] K. Izutsu, S. Kojima, *J. Pharm. Pharmacol.* **2002**, *54*, 1033.
[27] T. Scientific, NovexTM Pre-Cast gel electrophoresis guide USER GUIDE, https://www.thermofisher.com/document-connect/document-connect.html?url=https%3A%2F%2Fassets.thermofisher.com%2FTFS-Assets%2FLSG%2Fmanuals%2FMAN0003187_NovexPre-CastGelElectrophoresisGuide_UG.pdf&title=VXNlciBHdWlkZTogTm92ZXggUHJlLUNhc3QgZ2VsIGVsZWN0cm9waG9yZXNpcyBndWlkZQ== (accessed: April 2021).

[28] a) M. Adler, G. Lee, *J. Pharm. Sci.* **1999**, *88*, 199; b) M. Maury, K. Murphy, S. Kumar, L. Shi, G. Lee, *Eur. J. Pharm. Biopharm.* **2005**, *59*, 565; c) N. Y. Chew, H.-K. Chan, *Pharm. Res.* **1999**, *16*, 1098.
[29] Y. Y. Lee, J. X. Wu, M. Yang, P. M. Young, F. van den Berg, J. Rantanen, *Eur. J. Pharm. Sci.* **2011**, *44*, 41.
[30] K. J. Geh, M. Hubert, G. Winter, *Eur. J. Pharm. Biopharm.* **2018**, *129*, 10.
[31] E. Y. Shalaev, G. Zografi, *J. Pharm. Sci.* **1996**, *85*, 1137.
[32] J. H. Gitter, R. Geidobler, I. Presser, G. Winter, *J. Pharm. Sci.* **2018**, *107*, 2538.
[33] L. Weng, S. Ziaei, G. D. Elliott, *Sci. Rep.* **2016**, *6*, 28795.
[34] I. Gonda, A. F. Abdelkhalik, *Aerosol Sci. Technol.* **1985**, *4*, 233.
[35] F. Cardarelli, L. Digiacomo, C. Marchini, A. Amici, F. Salomone, G. Fiume, A. Rossetta, E. Gratton, D. Pozzi, G. Caracciolo, *Sci. Rep.* **2016**, *6*, 25879.
[36] J. S. Kim, T. J. Yoon, K. N. Yu, M. S. Noh, M. Woo, B. G. Kim, K. H. Lee, B. H. Sohn, S. B. Park, J. K. Lee, *J. Vet. Sci.* **2006**, *7*, 321.
[37] Y. Liu, O. Samsonova, B. Sproat, O. Merkel, T. Kissel, *J. Controlled Release* **2011**, *153*, 262.
[38] A. Ray, L. Cohn, *J. Clin. Invest.* **1999**, *104*, 985.
[39] S. M. Hoy, *Drugs* **2018**, *78*, 1625.
[40] S. Schüle, W. Frieß, K. Bechtold-Peters, P. Garidel, *Eur. J. Pharm. Biopharm.* **2007**, *65*, 1.
[41] C. Garcia-Galan, O. Barbosa, R. Fernandez-Lafuente, *Enzyme Microb. Technol.* **2013**, *52*, 211.